ISSN 1330-3651 (Print), ISSN 1848-6339 (Online)
https://doi.org/10.17559/TV-20240613001771
Original scientific paper

Effect of Material Composition and Machining Parameters on Surface Quality and Wear in CNC Turning of AA7075 using Taguchi Design

R. PARTHIBAN*, U. NATARAJAN, A. KUMARAVADIVEL

Abstract: This research examined the influence of cutting parameters on machining performance using Analysis of Variance (ANOVA) based on the Taguchi approach during CNC turning under wet conditions, employing AA7075 metal matrix and TNMG carbide inserts. Despite being an important characteristic, surface roughness was previously assessed due to its effect on the nose radius. Excellent surface finish quality may be produced with a machine working at high speeds, low feeds, and a big nose radius, achieving less than 0.718 μm. Thus, medium speeds and feed rate yielded poor material removal rates of 2.835 mm^3/min, while nose radius enlargement enhanced MRR. The given conditions showed a smooth layer due to this aspect. Medium speed, rapid feed rate, and 0.1 mm nose radius reduced Tool wear rate (TWRs). Benefits included extended tool life, improved surface finish, and reduced tooling costs. Additionally, the alloy with BN (5%) + WC (5%) plus Mg (1%) had the lowest wear rate. Those findings suggest a balanced machining process with increased productivity, better surface quality, and longer turning tool life. The research paper provides precise numerical data on the effects of material removal rate, surface roughness, and tool wear rate, which are crucial to process optimization for CNC turning of AA7075 metal matrix under wet conditions and TNMG carbide inserts.

Keywords: AA7075; CNC turning; metal removal rate; microstructure; surface roughness; tool wear rate

1 INTRODUCTION

Improvements in materials science and optimum design have been fuelled by the car industry's goal of lightweight design, fuel economy, and comfort. The development and widespread use of metal-matrix composites (MMCs), which provide better mechanical qualities and wear resistance than conventional lightweight metallic alloys like different grades of aluminum, have been sparked by this demand. MMCs, which are made up of a metallic matrix reinforced with three-dimensional inclusions like oxides, carbides, or nitrides, and usually mixed with elements like Al, Cu, Fe, Mg, Ti, or Pb, preserve the ductility of the metallic alloy while improving its modulus and strength. MMCs may be tailored to give better electrical, mechanical, and chemical characteristics, fulfilling the demanding requirements of modern engineering applications by carefully choosing the matrix material and reinforcements. These composites are excellent at withstanding high compressive and tensile stresses, transferring applied load from the ductile matrix to the reinforcing phase with efficiency.

Fabrication techniques like powder metallurgy, liquid metallurgy, and squeeze-casting are employed to incorporate reinforcement phases into the matrix, with inclusions ranging from continuous fibers to discontinuous particulates or whiskers. Particulate-reinforced composites, offering predictable isotropic behavior and lower manufacturing costs compared to fiber-reinforced counterparts, are gaining attention for their excellent mechanical, thermal, and tribological properties. Notably, aluminum-based PMMCs, particularly those containing silicon carbide (SiC) or alumina particles, exhibit enhanced wear resistance and thermal conductivity compared to the unreinforced matrix. These materials are used in calipers, connecting rods, brake rotors, pistons, and cylinder liners, among other automobile components. Under high contact loads, they delay the change from mild to severe wear and provide improved wear resistance. Aluminum-SiC PMMCs are being evaluated for use in car brake rotors, where they might replace traditional gray cast iron. The reinforced particle volume fractions of these PMMCs generally range from 10% to 30%. Furthermore, the production of automobile engine components uses hyper-eutectic Al-Si-based composites like A356 (Al, 7Si, 0.3Mg), which include Al2O3, ZrO2, or SiC particles. This illustrates how MMCs are adaptable and useful in the automotive and aerospace sectors.

In response to the need for greater fuel efficiency, automobile manufacturers are increasingly turning to alternative materials like metal matrix composites (MMCs). Utilizing MMCs for parts offers substantial weight savings while either maintaining or enhancing performance compared to traditional materials. Over the past decade, MMCs have steadily but gradually advanced towards widespread adoption in the automotive industry. To adhere to stricter standards for reduced fuel consumption, lower emissions, and enhanced efficiency, automakers are actively exploring alternative materials in their product designs. Advanced materials such as metal matrix composites (MMCs) represent a promising avenue for achieving notable enhancements in performance.

The microstructural characteristics, mechanical attributes, and wear behavior of AA matrix hybrid composites reinforced with graphite, alumina, and rice husk ash (RHA) were investigated by Alaneme and Sanusi [1]. A 6063 was used as the matrix substance. Alumina had particles less than 30 μm, but graphite and rice husk ash both had particles larger than 50 μm. Liquid metallurgy was used to create samples for different testing. The aluminum matrix's reinforcing particles were uniformly distributed, as shown by SEM micrographs. Hardness was shown to decrease with increasing concentrations of graphite and rice husk ash in all composites. On the other hand, the weight percentage of alumina and RHA rose with the tensile and yield strengths. Baradeswaran and Perumal [2] (2014) studied Al 7075/graphite composite wear and mechanical properties, helping us understand composite wear. Also, they studied Al 7075/Al2O3/graphite hybrid composites' mechanical and wear characteristics, showing the synergistic effects of numerous reinforcements.

Baradeswaran et al. [3] (2014) investigated the mechanical behavior, modeling, and optimization of wear parameters of B4C and graphite reinforced aluminium hybrid composites to increase their wear resistance for diverse applications. Deaquino-Lara et al. (2015) studied the tribological characteristics of mechanical alloyed and hot extruded Al7075-graphite composites to improve friction and wear knowledge. Wu et al. [4] (2014) examined how plasma activated sintering factors affected Al-7075/B4C composite microstructure and mechanical characteristics, improving our knowledge of sintering processes and composite materials. Deaquino-Lara [5] (2014) examined the structural characterisation of mechanical alloying and hot extruded aluminium alloy 7075-graphite composites, revealing production techniques and microstructures.

Lara et al. [6] conducted a tribological characterization of an aluminum/graphite composite produced through hot extrusion and mechanical alloying. They investigated the effects of milling time and graphite content on wear resistance and friction hardness. The graphite content varied from 0 to 1.5%, while the milling duration ranged from 0 to 10 hours. Wear resistance was tested using a pin and disc apparatus at sliding velocities of 0.367 m/s and normal loads of 20 and 40 N. Inspections of eroded surfaces and SEM analysis were also performed. The composite with 1.5% graphite concentration and a 10-hour milling period showed a uniform distribution of reinforcing particles and superior hardness and wear resistance compared to other extruded samples. The microstructure, mechanical attributes, and optical features of a composite reinforced with alumina nanoparticles based on aluminum 7075 were examined by Ezatpour et al. [7]. The conventional stir casting method was used to create the aluminum metal matrix composite. High porosity and insufficient reinforcing dispersion were noted at first. In order to avoid porosity, argon gas was introduced together with nano-sized Al2O3 into the molten aluminum 7075. Tensile and compression tests, hardness assessments, scanning electron microscopy, high-resolution transmission electron microscopy, and optical microscopy were used to assess mechanical behavior. The results showed that porosity is decreased via extrusion. Mechanical tests verified that the tensile strength, compression strength, and hardness were successfully increased by using Al2O3 nanoparticles and using an extrusion technique.

Flores-Campos [8] (2010) studied the microstructural and mechanical properties of 7075 aluminum alloy supplemented with silver nanoparticles to discover nanocomposites' strengthening processes. The composite materials literature overview includes several study issues, including their synthesis, mechanical characteristics, wear behavior, and microstructural characterisation. In 2015, Hernández-Martínez et al. [9] used ball milling to synthesize AA 7075-ZrO2 metal matrix nanocomposites, emphasizing powder technique and prospective applications. Jiang and Wang [10] (2015) examined the microstructure and mechanical characteristics of reformed cylindrical portions of 7075 aluminum matrix composite reinforced by nano-sized SiC particles, shedding light on nano-reinforced composites. Collectively, these studies significantly advance the field of composite materials, making important contributions to materials science and engineering. Karunesh G. et al.'s research [11] examined an Al2O3/AA 7075 composite's mechanical properties. Stir casting was used to create the samples, which had different weight percentages of Al2O3 at 0%, 1%, 3%, 5%, and 7%. A Brinell hardness tester was used to measure hardness. The tensile and compression strengths were also assessed. According to microstructural examination, the Al2O3 particles in the AA7075/Al2O3 composites were distributed uniformly. The findings showed that when the weight % of Al2O3 grew, the ultimate tensile strength and yield strength of the AA 7075/Al2O3 composite also reduced. Moreover, the percentage elongation decreased as the Al2O3 concentration increased. The results demonstrated that, up to a certain degree, toughness improved as fly ash content increased, whereas hardness and tensile strength dropped beyond that. The density of the composite decreased as fly ash content rose. Changes in the manufacture of fly ash and basalt ash reinforced Al 6061 composites and their mechanical characteristics are reported by Kumaravel S. et al. [12].

Mindivan et al. [13] (2007) researched squeeze cast aluminum matrix composites' tribological behavior, developing a better knowledge of their mechanical characteristics and performance. SEM examination was used to investigate RHA dispersion into AlSi10Mg. It was discovered that the ultimate tensile strength increased as the RHA content increased, reaching a peak at 12% before beginning to decrease. The weight % of RHA also boosted compressive strength, and larger RHA concentrations enhanced the composite's toughness. Hybrid composites of aluminum alloy (AlSi10Mg) reinforced with fly ash and rice husk ash (RHA) were reported by Narasaraju and Lingaraju [14]. In a similar vein, ductility increased when fly ash and RHA weight percentages increased but started to decline at the same composition. This pattern was also seen in hardness, which decreased at 10% fly ash and 10% RHA. Consequently, it was found that 10% fly ash and 10% RHA were the ideal ratios for this composite. The tribological characteristics of a stir-cast hybrid particulate metal matrix composite of Al7075 reinforced with Al2O3 and SiC were examined by Raghavendra and Ramamurthy [15].

Mediratta [16] evaluated the mechanical properties of the AA7075-Fly ash composite. The composite was made by a process called stir casting. In AA 7075, fly ash was treated with magnesium to increase its wetability by reducing its surface tension. The Charpy and Izod tests are used to determine the toughness of a produced composite. Saravanan and Kumar [17] reported on AlSi10Mg's reaction to reinforcement with RHA. Stir casting was the production technique, and various RHA weight percentages were used. The percentages of reinforcement weight were 3%, 6%, 9%, and 12%. AlSi10Mg was the matrix material used, and the size distribution of the reinforcement particles was 0.1-100 μm. 10% fly ash and 10% RHA, 15% fly ash and 5% RHA, and 5% fly ash and 15% RHA were the compositions used for reinforcement. The stir casting technique was used to create these specimens. Tensile strength rose when fly ash and RHA weight percentages climbed, but it began to decrease when fly ash and RHA weight percentages reached 10%. The composite material had different weight percentages of

Al2O3 (3%, 6%, 9%, and 12%) and 3% silicon carbide. As the weight % of reinforcement grew, the composite's density increased as well. Higher weight percentages of reinforcement enhanced wear resistance, according to wear tests performed using a pin-on-disc wear tester. A research on metal matrix composites of Al 6061/SiC and Al 7075/Al_2O_3 was carried out by Veeresh Kumar et al. [18], which added to our knowledge of these cutting-edge materials. The metals utilized as the basis elements for the composite are aluminum 6061 and 7075. SiC is added to aluminum 6061 in weight percentages of 2, 4, and 6% as well as 2%, 4%, and 6% to aluminum 7075. The piece was made using the stir casting process. It has been shown that microhardness and tensile strength increase with the weight % of reinforcing particle. It was shown that the AA7075/Al2O3 exhibited better mechanical properties than the Al 6061/SiC.

Perumal and Baradeswaran [19] looked on the mechanical characteristics and tribological characteristics of the graphite/AA 7075 composite. The samples were created by a traditional casting method, and heat treatment was then applied. An electric motor-driven impeller swirled the mixture for five minutes at 500 rpm. The composite had 5%, 10%, 15%, and 20% graphite compositions. Prior to testing, every sample was subjected to the T6 condition. Using a Rockwell hardness testing apparatus, a 100 kg weight was applied for the hardness test. Hardness was shown to decrease with an increase in graphite content. Using a pin-on-disc device, the wear test was carried out at room temperature (30 °C) at sliding speeds of 0.6, 0.8, and 1.0 m/s with applied pressures of 10, 20, and 30 N. As the composite's graphite content rose, the material's rate of wear reduced.

Bejaxhin et al. (2019) [20] conducted a study on Al6061 specimens subjected to stress, focusing on inspecting casting defects and the role of grain boundary strengthening. Their research utilized NDT methods in conjunction with scanning electron microscopy (SEM) micrographs to analyze the specimens. This study shed light on the relationship between casting defects, microstructure, and mechanical properties of Al6061 under stress conditions. In another study by [21] Brucely et al. (2022), the focus shifted towards hybrid composites, specifically AA8011-TiC-ZrB2. Using online acoustic emission measurement techniques, the researchers investigated the tensile strength and wear rate of the composite material. This research highlights the importance of real-time monitoring techniques in assessing the mechanical behavior of advanced materials, offering valuable insights into their performance characteristics. [22] Priya et al. (2022) explored wear studies on an Mg-5Sn-3Zn-1Mn-xSi alloy, employing the integrated response surface methodology (RSM) coupled with the genetic algorithm (GRGA) method for parameter optimization. By optimizing process parameters, the researchers aimed to enhance the wear resistance of the alloy. This research shows how optimization improves material characteristics and performance. Rao et al. [23] (2022) examined the wear behavior of aluminum matrix composites enhanced with h-BN and c-BN particles. By analyzing the samples, they examined the impact of boron nitride reinforcement on the composites' wear resistance, thereby contributing to the understanding of how reinforcing agents improve the mechanical properties of metal matrix composites. Additionally, Chandramohan et al. [24] (2023) explored the corrosion and wear behavior of Al-SiC composite materials, further advancing the knowledge in this field. Their study aimed to assess the performance of the composite under corrosive environments, providing valuable insights into its suitability for practical applications. Understanding the corrosion and wear behavior of composite materials is crucial for ensuring their reliability and durability in service.

The study used a design by Šarić et al. [25], and experiment to model and predict surface roughness in CNC turning, utilizing six cutting inserts and varying cutting parameters on a DMG Moriseiki-CTX 310 Ecoline lathe. A dataset of 750 instances was formed, with surface roughness measured for each sample, and Back-Propagation Neural Networks (BPNN) were employed for data analysis, evaluating RMS error across various network architectures. The study by Khelfaoui et al. [26] investigated the effects of tool nose radius, cutting speed, feed rate, and depth of cut on surface roughness, cutting temperature, and tool wear in intermittent turning of AISI D3 steel. Optimization using the desirability function and grey relational analysis methods is compared to improve performance parameters. Vukelić et al. and Milosevic et al. [27, 28], have discussed that the study explores the impact of cutting tool geometry on surface roughness in finish turning, utilizing three modeling techniques: Response Surface Method (RSM), Gaussian Process Regression (GPR), and Decision Tree Regression (DTR). It finds that GPR offers the best accuracy, emphasizing the importance of tool design for optimizing machining processes.

This study uses Taguchi and ANOVA to improve CNC turning parameters for AA7075 metal matrix composites containing Boron Nitride (BN), Tungsten Carbide (WC), and Magnesium (Mg) under wet machining conditions. This research examines how cutting speed, feed rate, and nose radius affect surface quality, material removal rate (MRR), and tool wear rate (TWR) while employing TNMG carbide inserts. Composite composition influences machining performance, especially with BN and WC for hardness and lubrication and Mg for weight reduction and microstructural improvement. A detailed literature review emphasises the necessity of understanding aluminium alloy and composite material microstructural features, mechanical properties, and wear behaviour. Recent metal matrix composite research has focused on advanced synthesis, tribological performance, and microstructural characterisation. These studies have improved composite manufacturing processes and mechanical and tribological qualities, allowing their use in aerospace, automotive, and other high-performance engineering fields.

2 MATERIALS AND METHODS

Based on previous literature, machining output parameters such as surface roughness, tool wear, and material removal rate are highly influenced by material composition and machining conditions. The combination of Al7075, Boron Nitride (BN), Tungsten Carbide (WC), and Magnesium (Mg) results in a composite with superior properties. Al7075 and WC provide high strength and

stiffness, while Al7075 and Mg contribute to weight reduction. BN and WC enhance wear and thermal resistance, and the overall blend improves mechanical and tribological performance, making the composite ideal for demanding applications like aerospace and automotive industries.

Aluminum alloy 7075 is renowned for its exceptional strength-to-weight ratio and is commonly used in aerospace, automotive, and structural applications. Its typical chemical composition falls within defined ranges to ensure consistent material properties. The alloy primarily consists of aluminum, with a minimum content specified to maintain its base properties. Other key elements include silicon (Si) within a maximum limit of 0.40%, iron (Fe) up to 0.50%, and manganese (Mn) typically not exceeding 0.30%. Copper (Cu) is a significant alloying element, ranging from 1.2% to 2.0%, contributing to the alloy's strength and corrosion resistance. Magnesium (Mg) content falls between 2.1% and 2.9%, enhancing both strength and machinability. Zinc (Zn) is present between 5.1% and 6.1%, aiding in strengthening the alloy through precipitation hardening. Trace amounts of titanium (Ti) up to 0.20% and chromium (Cr) up to 0.28% may also be present, contributing to grain refinement and improved corrosion resistance. This composition ensures that aluminum alloy 7075 exhibits the desired mechanical properties while meeting the stringent requirements of various high-performance applications.

Table 1 Typical chemical composition for aluminum alloy 7075

Element	%Present	
	Min	Max
Si	-	0.40
Fe	-	0.50
Cu	1.2	2.0
Mn		0.30
Mg	2.1	2.9
Zn	5.1	6.1
Ti	-	0.20
Cr	-	0.28
Al	Rem	-

Table 2 AL7075 mechanical properties

Density	2.8
Melting Point	660.2 °C
Modulus of Elasticity	68.3 GPa.
Thermal conductivity	0.57cal/Cms°C
Crystal Structure	FCC
Electrical resistivity	2.69

Aluminium alloy 7075, renowned for its high strength-to-weight ratio, boasts a density of 2.8 g/cm³, making it suitable for applications requiring lightweight yet robust materials. With a melting point of 660.20 °C, it maintains stability under elevated temperatures, which is crucial for aerospace and automotive industries. Its modulus of elasticity, measured at 68.3 GPa, highlights its ability to withstand deformation under stress while returning to its original shape upon release. The alloy's thermal conductivity of 0.57 cal/cm·s·°C facilitates efficient heat dissipation, essential for thermal management in various engineering applications. Featuring a face-centred cubic (FCC) crystal structure, the aluminium alloy 7075 exhibits favourable mechanical properties and is known for its excellent machinability and formability. Moreover, its electrical resistivity of 2.69 μΩ·cm makes it suitable for electrical conductivity applications, further broadening its utility across diverse industrial sectors.

Figure 1 Stir casting stages and Specimen preparation

Stir casting is advised for making a composite material from Al7075 reinforced with 1% tungsten carbide (WC), 1% boron nitride (BN), and 1% magnesium (Mg). The Al7075 alloy melts at 477 °C to 635 °C; however, it is usually heated to 700 °C to 750 °C for casting and fluidity. The alloy is entirely melted and ready for reinforcing at this temperature. Hold the material for 5-10 minutes after reaching the melt temperature. This holding period is necessary to establish a homogeneous temperature distribution and enable additional components like magnesium to alloy with the base metal and improve ceramic reinforcement wettability.

Table 3 Properties of boron nitride

Thermal properties	Thermal conductivity	300+	w/m-k
	Specific heat	794	J/kg-k@25c
	Thermal density	2.25	g/cc
Electrical conductivity	Dielectric constant	-	-
	Volume resistivity	10^{i5}	Ohm-cm
Mechanical Property	Young's modulus	40	Gpa
	Knoop hardness	11	Kg/mm2
	Mohr's hardness	< 2	

Mixing Ratio

Sample 1: Al7075 + WC+1% +BN 1% +Mg-1%

Sample 2: Al7075 + WC+3% +BN 3% +Mg-1%

Sample 3: Al7075 + WC+5% +BN 5%+Mg-1%

Preheat the WC and BN particles to 300°C to 400°C before adding them. Removing moisture that might cause porosity and improving particle wettability and dispersion in the molten matrix is crucial. Before adding reinforcements, magnesium should be added directly to molten Al7075 to increase wettability. Stir casting requires a mechanical stirrer with a graphite or ceramic-coated impeller for stirring. Stirring should last 5-10 minutes at 400–600 rpm. To achieve equal distribution, warmed WC and BN powders are gently injected into a visible vortex in the melt while stirring. To reduce oxidation, the procedure may be done in argon or nitrogen for best results. After

evenly mixing the reinforcements, pour the composite melt into warmed moulds at 200 °C to 300 °C. This reduces thermal stress and cast product flaws like porosity and fractures. Controlled melting, preheating, stirring, and casting create a homogenous composite with improved mechanical and thermal qualities. Sample compositions were created by blending numerous components. Sample 1 included Al7075 alloy, 1% tungsten carbide (WC), 1% boron nitride (BN), and 1% magnesium (Mg).

In Sample 2, WC and BN were raised to 3% each while magnesium remained 1%. Finally, Sample 3 has 1% WC, BN, and magnesium like Sample 1. These mixing ratios were chosen to obtain desirable material qualities, since WC and BN concentrations may affect strength, hardness, and thermal conductivity. The inclusion of magnesium likely improved characteristics or processing. Each sample's composition is carefully balanced to satisfy application-specific performance requirements. The HRB value below was determined by using a Shivganga testing equipment to measure hardness. The Ratio-3 displays the highest hardness.

Table 4 Mixing ratio-total Al 7075-1080 gram

Ratio	AL 7075 / grams	WC-% / grams	BN-% / grams	Mg 1% / grams
1	360	3.6 (1%)	3.6 (1%)	3.6
1	360	11(3%)	11(3%)	3.6
1	360	18 (5%)	18 (5%)	3.6

Table 5 Hardness value of hybrid AMMC

S. No	Composition	Hardness / HRB
R_1	Al7075+WC+1%+BN1%+Mg-1%	78
R_2	Al7075+ WC+3%+BN 3%+Mg-1%	82
R_3	Al7075+ WC+5%+BN5%+Mg-1%	88

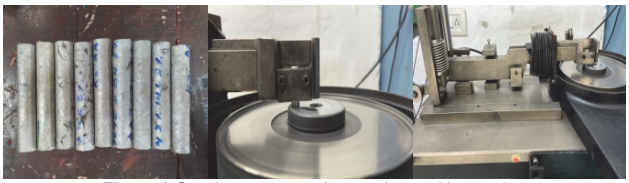

Figure 2 Specimen preparation, testing and inspection

The hardness of hybrid aluminum matrix metal composites is shown in Tab. 5. Al7075 alloy containing 1% tungsten carbide (WC), boron nitride (BN), and magnesium (Mg) has 78 HRB hardness. R2, with 3% WC and BN and 1% magnesium, has 82 HRB hardness. R3 had the greatest hardness, 88 HRB, because of its 5% WC, BN, and 1% magnesium reinforcements. These results show a positive association between hybrid AMMC hardness and reinforcing element concentration, indicating that careful composition management may tune material attributes to satisfy engineering performance requirements.

3 EXPERIMENTAL PROCEDURE

Experimental design can become overly complex for common usage, particularly when process parameters increase, necessitating a large number of tests. To address this challenge, the Taguchi technique utilizes orthogonal arrays to explore the entire parameter space with minimal trials. By calculating a signal-to-noise (S/N) ratio from experimental data, this method quantifies quality characteristics that deviate from intended levels. Typically, the lower, higher, and nominal quality parameters are utilized to assess the S/N ratio. S/N analysis involves comparing the S/N ratio of each process parameter. Quality characteristics improve with a higher S/N ratio, regardless of category.

Thus, the best process parameter level which has been mentioned in the Tab. 6 has the highest S/N ratio. Statistically significant S/N and ANOVA analysis may predict the best process parameter combination. Finally, a confirmation experiment verifies the parameter design-derived optimum process parameters. Three Signal-to-Noise ratios are important for static problem optimization. To enhance experiment quality, signal to noise ratio formulas allow the experimenter to always use the biggest factor level option. We calculated the Signal-To-Noise ratio for quality.

Table 6 Process parameters and variables as per the L9 array experimental design

S. No.	Spindle Speed / RPM	Feed / mm/Rev	Nose radius / mm
1	500	0.050	0.02
2	500	0.075	0.04
3	500	0.100	0.08
4	750	0.050	0.04
5	750	0.075	0.08
6	750	0.100	0.02
7	1000	0.050	0.08
8	1000	0.075	0.02
9	1000	0.100	0.04

In the experimental setup, a Batliboi Smarturn CNC lathe was employed to machine work specimens composed of AA6082 alloy reinforced with tungsten carbide (Wc) and silicon carbide (SiC), with dimensions set to Φ25mm (diameter) × 100 mm (length). Cutting was executed using Carbide-TAEGUTEC-TT-5100-04 inserts (TNMG 120404-HACNM6431 PC9030) known for their hardness and wear resistance. Notably, no coolant was used during machining, possibly to assess dry cutting conditions' impact on tool performance. Metal removal rate was calculated via weight measurement, while machining time was directly recorded from the CNC machine. This meticulous arrangement allowed for systematic evaluation of machining efficiency and facilitated parameter optimization to enhance productivity and tool life.

Figure 3 Experimental setup of CNC turning machine (Batliboi Smarturn CNC lathe) and the machined specimens

The presented data are obtained from a machinery practice considered on a lathe or similar machining equipment types. The data in the table relates to a particular interplay of rotation speed (RPM) and feed movement (mm/Rev). It is revealed in the table by the figure along with several other findings of relevance. The results of the experiments are standardized machining time per part, tool wear rate, surface roughness average, and material removal rate. Lathe Machine Flat Bed CNC Lathe Batliboi Smarturn CNC lathe. Maching has been used for this machining operation.

Investigating the data, we reveal some different patterns. For the first aspect, there is also a reduction of machining time per piece with the increase of the spindle speed and feed rate that is related to the better operation of the material removal process. Nevertheless, the cost of this efficacy in the form of high wear rate of cuts and feeds is notable. Likewise, it happens frequently that the lower roughness average number is achieved eventually, while the velocity and feed rate are high. Additionally, the material removal rate typically grows along with the speed/feed rate which are converted to e.g. higher volumes of material removed per unit of time or reduced manufacturing time. Tab. 8 shows how the tool wear rate (TWR) in machining changes when the radius of the tool's nose is different. The nose radii tested were 0.02, 0.04, and 0.08. There are three sets of data, each with before and after weights of the tool and the resulting TWR in grams. An analysis shows that different nose radii affect TWR in different ways. For example, with a nose radius of 0.02, the before and after tool weights are 3.24 and 3.2318 grams, giving a TWR of 0.0082 grams. Similar patterns of TWR variation occur with nose radii of 0.04 and 0.08, based on how the before and after weights change.

Table 7 Experimental data analysis

SL. NO	SPEED (*N*)(RPM)	FEED / mm/Rev	NR / mm	MT / min	TWR / gm	RA / µm	MRR mm^3/min
1	500	0.050	0.02	3.27	0.0082	0.887	1.243554
2	500	0.075	0.04	2.41	0.0076	1.097	1.029098
3	500	0.100	0.08	2.18	0.0088	1.029	1.902569
4	750	0.050	0.04	2.40	0.0013	0.813	1.760455
5	750	0.075	0.08	2.10	0.0005	1.188	1.702688
6	750	0.100	0.02	1.55	0.0009	1.864	2.835377
7	1000	0.050	0.08	2.15	0.0007	0.718	1.685403
8	1000	0.075	0.02	1.59	0.0109	1.148	2.490195
9	1000	0.100	0.04	1.44	0.0111	1.006	2.014145

For example, in Tab. 7, considering the data for the first row, where the spindle speed is 500 RPM and the clamping rate is 0.050 mm/Rev, we concluded that the machining time per piece is 3.27 minutes, the tool wear rate equals 0.0082 grams per minute, the surface roughness mean is 0.887 µm These numerical demonstrations give useful clues to manufacturers to figure out how adjustments in machining parameters affect not only efficiency but also quality of machining process and this helps in improvement of production at large scale and better product quality.

Table 8 Tool wear rate (before and after each process in Mg)

Nose Radius / mm	0.02			0.04			0.08		
Before Weight / grams	3.24	3.2318	3.2309	6.46	6.4524	6.4511	6.87	6.8612	6.8607
After Weight / grams	3.2318	3.2309	3.22	6.4524	6.4511	6.44	6.8612	6.8607	6.86
TWR / grams	0.0082	0.0009	0.0109	0.0076	0.0013	0.0111	0.0088	0.0005	0.0007

Table 9 Tool wear rate and S/N ratios values for the experiments

TRIAL	DESIGN	SPEED / rpm	FEED / mm/Rev	NR / mm	TWR / Gms/min	SNRA1
1	$A_1B_1C_1$	500	0.050	0.02	0.0082	41.7237
2	$A_1B_2C_2$	500	0.075	0.04	0.0076	42.3837
3	$A_1B_3C_3$	500	0.100	0.08	0.0088	41.1103
4	$A_2B_1C_2$	750	0.050	0.04	0.0013	57.7211
5	$A_2B_2C_3$	750	0.075	0.08	0.0005	66.0206
6	$A_2B_3C_1$	750	0.100	0.02	0.0009	60.9151
7	$A_3B_1C_3$	1000	0.050	0.08	0.0007	63.0980
8	$A_3B_2C_1$	1000	0.075	0.02	0.0109	39.2515
9	$A_3B_3C_2$	1000	0.100	0.04	0.0111	39.0935

This table provides an overall picture of tool life rate (TWR) and Signal-to-Noise Ratios (SNR) coming out from slices of experiments performed using various design conditions. Each trial is divided by a special combination of A, B and C factors, which are labeled to identify the particular operating parameters group together as shown in the table 9. Such factors involve spindle speed (Speed) which is a unit in revolutions per minute (RPM). Furthermore, feed rate (Feed) is in millimetres per revolution (mm/Rev). Lastly, normalised chip thickness (NR) refers to the thickness of material removed per millimetre beyond the cutting edge. The TWR values are represented in the grams which display the rate at which the cutting tool wears out during the machining process, and, the SNR on the other hand, provide information about the quality of the cutting tool in terms of how good or bad the machining process was. What resulted was not randomness but an observable repetition of specific trends. Primarily, the TWR influence by several design parameters reveals as is the case. Trial by trial speed, feed rate and chip thickness variation assists in detecting tool wear rates which is also comparably affected. Further, the spindle speed and feed rate are typically the principal factors that affect TWR. The increase in the rate of machining often results in the reduction of TWR while the reduction of machining rate often results in the TWR increase

Additionally, the variability in SNR of different setups can help us discover the type of machining result we can realize after the experiment. Values of SNR which are higher, show excellent performance, so those combinations of design variables from which more effective machining outcomes will be, are highlighted with these. Further, as case for example 5 (A2B2C3) with speed of 750 RPM, feed rate of 0.075 mm/Rev, and chip thickness of 0.08 is

concerned, its SNR of 66.0206 indicates that machining process of such a nickel alloy sample is optimally performed. Eventually, the gathered information will be a useful tool for manufacturers working to upgrade their machining practices.

Figure 4 Evaluation of removal rates of tool and workpiece of CNC turned specimen

Determination of the removal rate for the examined tool and work piece by balancing the parts' weight after machining with a CNC machine is a significant stage in the machining process. This process helps in achieving good quality control and is essential for improving the machining process. This method, commonly known as tool is a technique to measure weight of a cutting tool before and after machining of the workpiece to deduce the amount of material removed during machining mentioned in the Fig. 4. Before this drop-weight machining is started, the precise weight of the tool is measured, which is recommended to serve as a reference point for the weight comparison purpose.

After applying the CNC turning process with specified parameters, the cutting tool that has been engaged in the process progressively removes material from the workpiece until its desired dimensions are attained. Finished with the machining process, the tool is withdrawn and weighed again. This is done via the same exacting devices used at the start of the operation. Meanwhile, machine weighs the part to be machined along with the record. This is accomplished by simply subtracting final weight of the tool from its original weight, with the amount of material worn-away from the tool being thus known. The same way, the difference in weight between the texture's initial weight and its final on the workpiece tell us how much of the material is driven out of the workpiece.

The planned material allowances for the tool and the workpiece are computed, making estimates of the material being taken out of both the tool and the workpiece, and as the results are evaluated the efficiency and effectiveness of the machining process is therefore assessed. Dissonances in the removal rate of actual and set result can be considered as a consequence of issues like tool wear, cutting tool defects, improper machining parameters, or nonconstant material qualities. Data from the evaluation will be analyzed to consider parameters like adjustment to machining or tool selection in order to make changes that bring better efficiency, accuracy, and quality of the process. With the help of these modifications, access is provided to diminish the tool, intensify material removal speed and improve the surface finish rate that does not compromise dimensional precision.

Stylus probe surface roughness measurements in CNC turning samples are a reliable approach to evaluate machined surfaces. After fixing the sample, the stylus probe is calibrated for scanning. Process circumstances and surface polish requirements can affect measurement parameters like cutoff length and sample length. The CNC machine uses a height measuring probe to measure stage deformations and level steps. Data acquisition turns analog probe signals into digital data for analysis. Software for typing metrics like *Ra* and *Rz* reveal surface imperfections quantitatively. Interpreting this parameter may aid quality control and machining parameter modification. Auditable data will be utilized to enhance or minimize any organization procedure. Validating and calibrating the sensor and measuring system periodically preserves measurement accuracy over time. These procedures will let the inspector assess CNC turning surface roughness effectively for quality control and productivity.

Figure 5 Measurement of stylus probe used for surface roughness testing

4 RESULTS AND DISCUSSION

By looking into the information, we see that the experiments deal mostly with cutting conditions like turning and milling. The Tab. 10 includes the variables section that is presented as (speed-RPM), feed-(mm/Rev), net removal (NR) in millimetres, machining time (MT) in minutes, tool wear rate (TWR) in grams, surface roughness (RA) in microns, and material removal rate (MRR) in cubic millimetres per minute. The experiment is carried out in this way by measuring different speeds and feeds while minimizing the quantity of feed. These parameters such as material removal rate, surface roughness, are analyzed for every combining of processes as machining procedures are implemented subsequently. This experimental method helps researchers in that they are well enough to witness and analyze how the surge of feed and speed influences the process of machining and its outcomes. These variables are altered in such a manner that researchers can analyze the data and thus develop the best operational scenarios for increased efficiency, quality and performance. With the aim of adding clarity or explicit goals of the experiment more technically oriented and data-giving individuals will be able to grasp meaning and analyze outcomes.

Table 10 Experimental data analysis and outcomes

SL. NO	SPEED (*N*) (RPM)	FEED / mm/Rev	NR / mm	MT / min	TWR / gm	RA / micron	MRR / mm^3/min
1	500	0.050	0.02	3.27	0.0082	0.887	1.243554
2	500	0.075	0.04	2.41	0.0076	1.097	1.029098
3	500	0.100	0.08	2.18	0.0088	1.029	1.902569
4	750	0.050	0.04	2.40	0.0013	0.813	1.760455
5	750	0.075	0.08	2.10	0.0005	1.188	1.702688
6	750	0.100	0.02	1.55	0.0009	1.864	2.835377
7	1000	0.050	0.08	2.15	0.0007	0.718	1.685403
8	1000	0.075	0.02	1.59	0.0109	1.148	2.490195
9	1000	0.100	0.04	1.44	0.0111	1.006	2.014145

The table shows the source of error, kind and level, as well as their value for the design of the experiment. Through its structure, it puts the vital data for research activities in place in a manner suited to the stepwise nature of an experiment. We start with a column named "Factor" which tags variables that are under investigation that include "SPEED," "FEED" and "NR." They are parameters or conditions that experimentalists always stay in control with or manipulate over the process. Additionally, the "Type" column differentiates their types of costing as fixed or variable costs. In this situation, all factors CRS, DWR, and NRI have established a stage where their levels are fixed or known and stay constant through the experiment.

Definitely, the aforementioned class defines the basis for maintaining the consistency and complying with the experimental settings. Another, the "Levels" column means total of the levels in respect of every factor. Following that, SPEED rate has 3 versions (500, 750, and 1000 RPM), which is applicable to the FEED and NR controller with 3 levels of specifications too. They give clues about loci associated with these traits thereby revealing the range of values for these factors. The latter one, known as the "Values" column, shows the exact numerical values or levels corresponding for each index. Taking SPEED ranges- which are RPM values (500,750, and 1000) as an example, other levels like FEED and NR are indicated by mm/Rev values. These values represent the boundaries within which the three branches of microscopy operate.

Table 11 (i) Response table for SN Ratio of Tool Wear Rate (TWR) and (ii) Analysis of Variance for TWR, using Adjusted SS for Tests

(i)	LEVEL	SPEED	FEED	NR
	1	41.74	54.18	47.30
	2	61.55	49.22	46.40
	3	47.15	47.04	56.74
	DELTA	19.81	7.14	10.34
	RANK	1	3	2

(ii)	Source	Df	Seq Ss	Adj Ms	F	P	% of Contribution
	SPEED	2	0.000098	0.000049	3.49	0.223	38
	FEED	2	0.000021	0.000011	0.76	0.567	30
	NOSER	2	0.000022	0.000011	0.79	0.559	22
	Error	2	0.000028	0.000014			10
	Total	8	0.000170				100

In the given scenario, the system design A2B2C3 has achieved the minimum tool wear rate (TWR) of 0.0005 grams at a rotational speed of 750 RPM and a feed rate of 0.075 mm/rev. The statement identifies rotational speed (SPEED) as the primary influencing factor and nose radius (NR) as the secondary influencing factor on TWR. This assertion can be justified through careful analysis of the role each factor plays in the machining process. Rotational speed (SPEED) holds a primary influence due to its direct impact on cutting speed and the resultant heat generation at the cutting edge. At higher speeds, the cutting tool encounters increased frictional forces and thermal stresses due to greater contact with the workpiece material. This heightened friction and heat can accelerate tool wear, leading to a higher TWR. Conversely, lower speeds may result in insufficient cutting action. The observation that the system design A2B2C3 achieves the minimum TWR at 750 RPM suggests that this specific rotational speed is optimal for minimizing tool wear under the given cutting conditions.

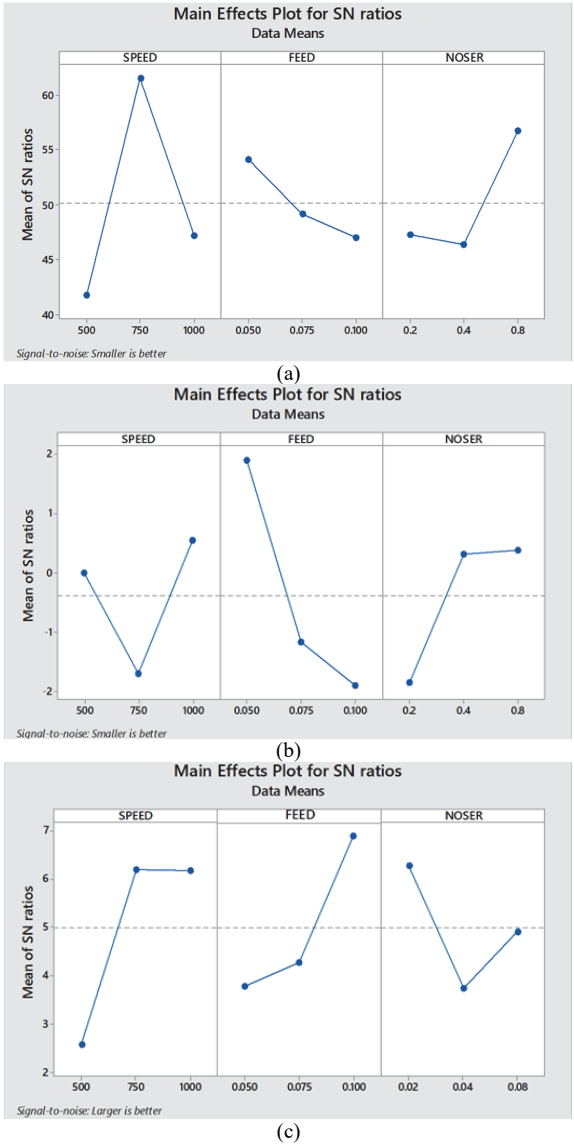

Figure 6 Main effects plot of (a) tool wear rate; (b) surface roughness; (c) material removal rate

In the evaluation of manufacturing performance parameters such as surface roughness, material wear rate, and machining time, different optimisation criteria are applied based on the desired outcomes, following Taguchi's approach. Surface roughness is assessed using the "lower is better" criterion because a smoother surface is typically preferred for improved functionality and aesthetics; thus, minimising roughness is the goal. For material wear rate, the "Higher the Better" criterion is applied when considering the material's resistance to wear; higher values in this context indicate better wear performance and durability, which are desirable traits in engineering applications. Machining time, on the other hand, is optimised based on the "Nominal the Better" principle, where the objective is to achieve a specific target value. We seek an optimal balance because too short a machining time can compromise quality, while too long can reduce efficiency and increase costs. These tailored criteria ensure accurate evaluation and optimisation of each parameter while aligning with functional and performance requirements in the manufacturing process.

Nose radius (NR) emerges as a secondary influencing factor, primarily shaping the distribution of cutting forces and stress concentration at the tool-workpiece interface. A larger nose radius disperses cutting forces over a broader area, reducing localized stresses and, consequently, mitigating tool wear. Conversely, a smaller nose radius may concentrate forces, leading to more rapid wear. Although rotational speed exerts the primary influence on TWR, the specific nose radius (C3) in the A2B2C3 design likely optimizes the tool's geometry to further minimize wear. The fact that this design exhibits the lowest TWR compared to designs with different nose radii underscores the significance of nose radius in influencing tool wear, albeit to a lesser extent than rotational speed as mentioned in the Tab. 12.

Table 12 (i) Response table for SN Ratio of Surface roughness (SR) (ii) Analysis of Variance for RA, using Adjusted SS for Tests

(i)	LEVEL	SPEED	FEED	NR
	1	–0.00364	1.90574	–1.85541
	2	–1.70235	–1.16643	0.31403
	3	0.54224	–1.90306	0.37762
	DELTA	2.24459	3.80880	2.23303
	RANK	2	1	3

(ii)	Source	Df	Seq Ss	Adj Ms	F	P	% Of Contribution
	SPEED	2	0.19243	0.09621	2.06	0.327	22
	FEED	2	0.38230	0.19115	4.09	0.196	44
	NR	2	0.21066	0.10533	2.26	0.307	24
	Error	2	0.09340	0.04670			10
	Total	8	0.87879				100

The milling operation has such parameters as the rate of tool wear, the average roughness, and the material left over, which define the efficiency and quality of the operation. Then, for tool wear rate analysis the parameter combination (A1 - speed 500 RPM, B3 - feed 0.1 mm/Rev, and C2 - nose radius 0.04 mm) is carefully evaluated. A simultaneous combination of testing tool wear and use with environmental conditions helps in understanding the machine degradation rate.

Table 13 Response table for SN Ratio of Metal Removal Rate (MRR) and Analysis of Variance for MRR, using Adjusted SS for Tests

(i)	LEVEL	SPEED	FEED	DOC
	1	2.576	3.780	6.290
	2	6.196	4.266	3.748
	3	6.180	6.907	4.915
	DELTA	3.619	3.127	2.542
	RANK	1	2	3

(ii)	Source	Df	Seq Ss	Adj Ms	F	P	% of Contribution
	SPEED	2	0.9532	0.4766	4.02	0.199	38
	FEED	2	0.7644	0.3822	3.22	0.237	30
	NR	2	0.5543	0.2771	2.34	0.300	22
	Error	2	0.2372	0.1186			10
	Total	8	2.5090				100

Furthermore, cut strides average roughness parameters A2 (speed - 750 RPM), B1 (feed - 0.25 mm/Rev) and C3 (nose radius - 0.08 mm) are taken as a measurement. Therefore, the combination of these parameters gives information not only about surface injuries left over after cutting but also helps to understand the product quality level provided. In addition, spindle speed (500 R.P.M.) and feed (0.075 mm/Rev) rate are defined as parameters A1 and B2, respectively, while C3 (nose radius - 0.08 mm) is another variable that contributes to the improvement of the material removal rate.

Table 14 Metal removal rates after and before machining

Before Weight	83.84	81.77	83.56	85.71	81.76	84.60	81.46	83.35	78.09
After Weight	72.82	72.26	72.32	74.26	72.07	72.69	71.64	72.62	70.23
MT	3.27	3.41	2.18	2.40	2.10	1.55	2.15	1.59	1.44

$$\textit{TWR} = 0.00556 + 0.00264\ \text{SPEED\_500} - 0.00466\ \text{SPEED\_750} + 0.00201\ \text{SPEED\_1000} - 0.00216\ \text{FEED\_0.050} + 0.00078\ \text{FEED\_0.075} + 0.00138\ \text{FEED\_0.100} + 0.00111\ \text{NOSER\_0.2} + 0.00111\ \text{NOSER\_0.4} - 0.00222\ \text{NOSER\_0.8} \quad (1)$$

$$\textit{RA} = 1.0833 - 0.079\ \text{SPEED\_500} + 0.205\ \text{SPEED\_750} - 0.126\ \text{SPEED\_1000} - 0.277\ \text{FEED\_0.050} + 0.061\ \text{FEED\_0.075} + 0.216\ \text{FEED\_0.100} + 0.216\ \text{NOSER\_0.2} - 0.111\ \text{NOSER\_0.4} - 0.105\ \text{NOSER\_0.8} \quad (2)$$

$$\textit{MRR} = 0.1858 - 0.0181\ \text{SPEED\_800} + 0.0079\ \text{SPEED\_1000} + 0.0102\ \text{SPEED\_1200} - 0.0448\ \text{FEED\_0.025} - 0.0351\ \text{FEED\_0.050} + 0.0799\ \text{FEED\_0.075} - 0.0341\ \text{NR\_0.2} + 0.0179\ \text{NR\_0.4} + 0.0162\ \text{NR\_0.8} \quad (3)$$

This fact helps in the accurate machining process and higher material removal rate, as the set quality standards are attained. In this regard, producers may carefully examine the influence that selection of these factors and their interaction on machine tools could perform, both enhancing good quality and optimizing productivity. As such, producers may be able to tweak their machining procedures to improve efficiency, product quality, and productivity at the same time ensuring that they are competitive.

The figures obtained for contribution of process parameters gain the importance of such aspect that particular parameter could over-weight the final result of process in machining. In the context provided, three key parameters are evaluated: the tool wear rate, the surface

roughness, and the rate of material removal represent critical performance parameters. Firstly, among those factors that contribute to the tool wear rate, the speed factor stands out and amounts to 58%. This shows that speed at which machining process is being carried out plays the major role in determining the grade of tool worn out with time. The wear and friction may be risen by a higher speed which may not be good for other matters during the process while the reduced wear at low speed may not fit well in general. The other contributory factor is the feed extent that has the biggest sway with a 44% contribution. The statistic reveals that the way the tool is capable to have the rate of advancement per lap has a large number of effects on the quality of finished surface. A smaller feed more often produces a velvety smooth surface but a larger feed will be rough due to the increased engagement between the work piece and the tool resulting in the removal of bigger volume of the material. On the other hand, as far as material removal rate is concerned, speed corresponds and has the largest role, 58%.

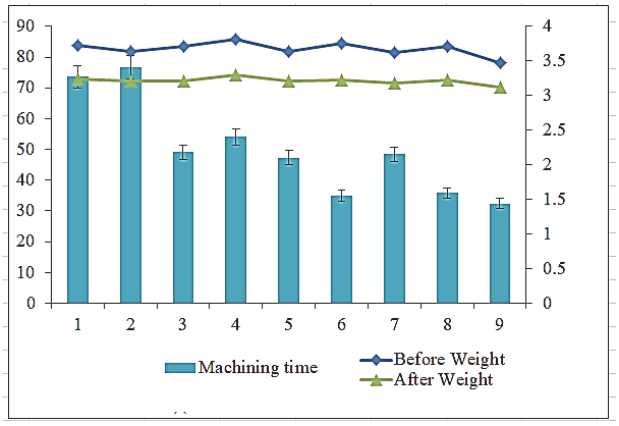

Figure 7 Material removal rate (mm³/min) and machining time (min)

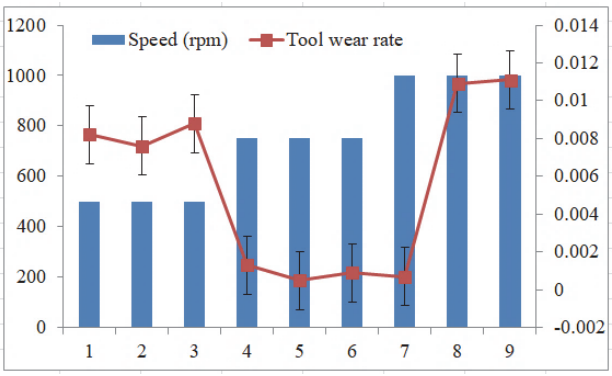

Figure 8 Relation between Speed (rpm) and tool wear rate (Grams/min)

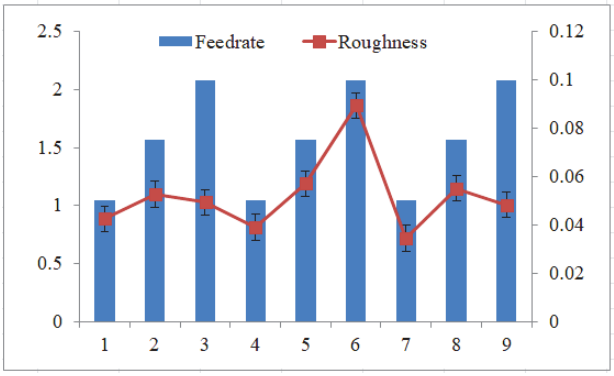

Figure 9 Correlation of feedrate (mm/rev) and surface roughness (μm)

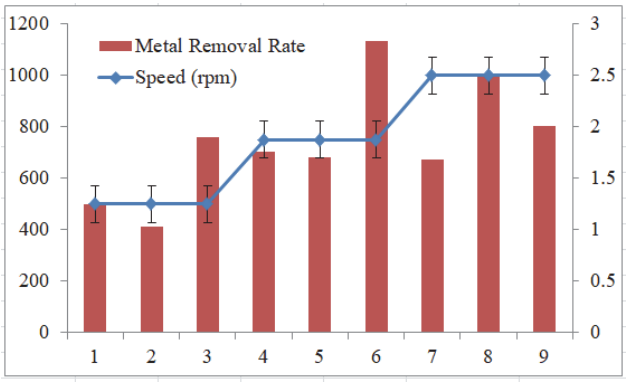

Figure 10 Influence of speed (rpm) on metal removal rate (mm3/min)

The interaction between various machining parameters and output responses is illustrated through Figs. 7 to 11. Fig. 7 demonstrates the inverse relationship between material removal rate (MRR) and machining time, indicating that higher MRR corresponds to reduced machining time, thus improving productivity. Fig. 8 highlights how increasing cutting speed affects the tool wear rate, showing a tendency for wear to accelerate at higher speeds due to elevated thermal and mechanical stresses. Fig. 9 presents the correlation between feed rate and surface roughness, revealing that higher feed rates generally lead to increased surface roughness, thereby affecting surface quality. Fig. 10 further emphasizes the influence of cutting speed on MRR, where optimal speeds enhance metal removal efficiency without compromising tool integrity.

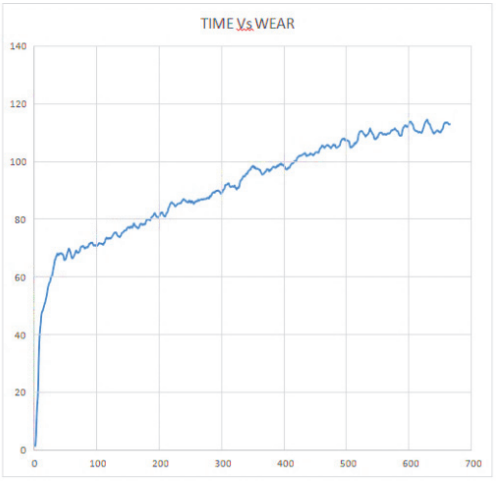

(a)

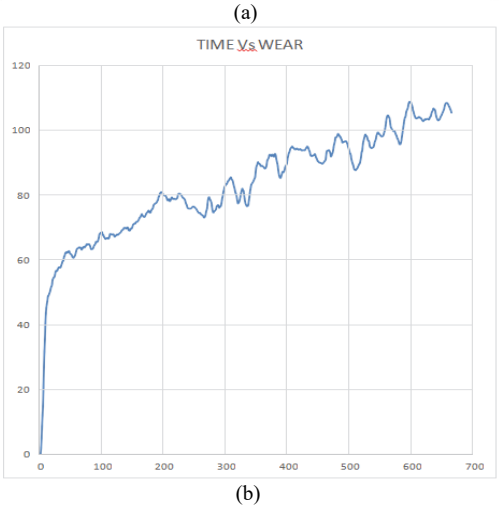

(b)

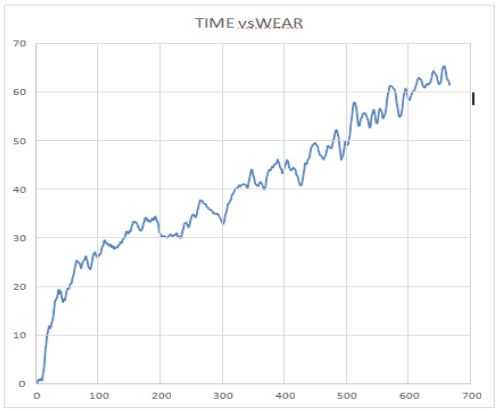

(c)

Figure 11 Time-VsWear rate of Wear Test samples; (a) Ratio-1, (b) Ratio-2 and (c) Ratio-3. (At a speed of 717 RPM, with a normal load of 15 N, and a pin diameter of 10 mm, the sliding distance covered is 1000 mm)

Finally, Fig. 11 illustrates the time-dependent wear behavior of different composite ratios during wear tests conducted at a constant speed of 717 RPM, under a normal load of 15 N, with a pin diameter of 10 mm over a sliding distance of 1000 mm. Subfigures (a), (b), and (c) compare wear rates across Ratio-1, Ratio-2, and Ratio-3, showing how varying composite compositions influence wear resistance over time. These interactions collectively demonstrate the complex relationship between process parameters, material properties, and performance outcomes in machining AA7075-based composites.

The fact that these speed rates will greatly affect the process rate of material elimination only goes on to emphasize the meaning of timing during the production. Sufficient spindle speeds which facilitate the faster removal of the material may not be the best fit in some cases as it should be tempered by tool life and surface quality. Comprehending the contributions of the process parameters to the accuracy levels allows machinists to identify the most audit mechanisms and to use them in the best ways possible. Supporting parameters on higher contribution rates may be of help for both tool wear rate and material removal rate. Therefore, based on the defined outputs, manufacturing processes can be tailored with minimizing the potential adverse effects. Optimization of parameters is a complex situation; hence it plays a critical role in production, efficiency of the machines, and in guaranteed product quality of the machining operations.

SEM Identification of roughness and removal rates

Al7075, a renowned aluminum alloy prized for its superior strength-to-weight ratio and corrosion resistance, forms the matrix of this composite. Typically exhibiting a fine grain structure, Al7075 hosts various alloying elements like zinc, magnesium, and copper. Into this matrix, tungsten carbide (WC) is integrated as reinforcing agents, renowned for their hardness and wear resistance. These WC particles, dispersed throughout the aluminum matrix, bolster the material's hardness and resilience.

Boron nitride (BN), recognized for its exceptional thermal conductivity and chemical stability, is introduced as an additive, potentially enhancing the composite's thermal properties or lubrication characteristics. Within the microstructure, one would expect to find dispersed BN particles embedded within the aluminum matrix. Additionally, magnesium (Mg) is incorporated as an alloying element, contributing to the composite's strength and corrosion resistance. The microstructure likely reveals the presence of magnesium-containing phases or precipitates, further fortifying the material's mechanical properties. In essence, the composite's microstructure presents a sophisticated amalgamation of aluminum matrix, tungsten carbide reinforcements, boron nitride additives, and magnesium alloying elements, each meticulously tailored to impart desired mechanical, thermal, and chemical attributes. Thorough analysis utilizing advanced microscopy techniques such as scanning electron microscopy (SEM) and transmission electron microscopy (TEM) is crucial for uncovering and characterizing the intricate microstructural details of this composite material. Increasing the composition of tungsten carbide (WC) and boron nitride (BN) in the Al7075 composite can have notable effects on both surface roughness and removal rates during machining processes. As the concentration of tungsten carbide increases, the surface roughness of the machined component tends to decrease. This is primarily due to the enhanced hardness and wear resistance imparted by WC particles, reducing the tendency for tool wear and deformation during machining, resulting in smoother surface finishes. Similarly, the addition of boron nitride can lead to improvements in surface roughness. BN's lubricating properties reduce friction and heat generation during machining, resulting in reduced tool wear and improved surface finish. Additionally, BN particles may act as a solid lubricant, facilitating smoother chip formation and evacuation, further contributing to a finer surface finish.

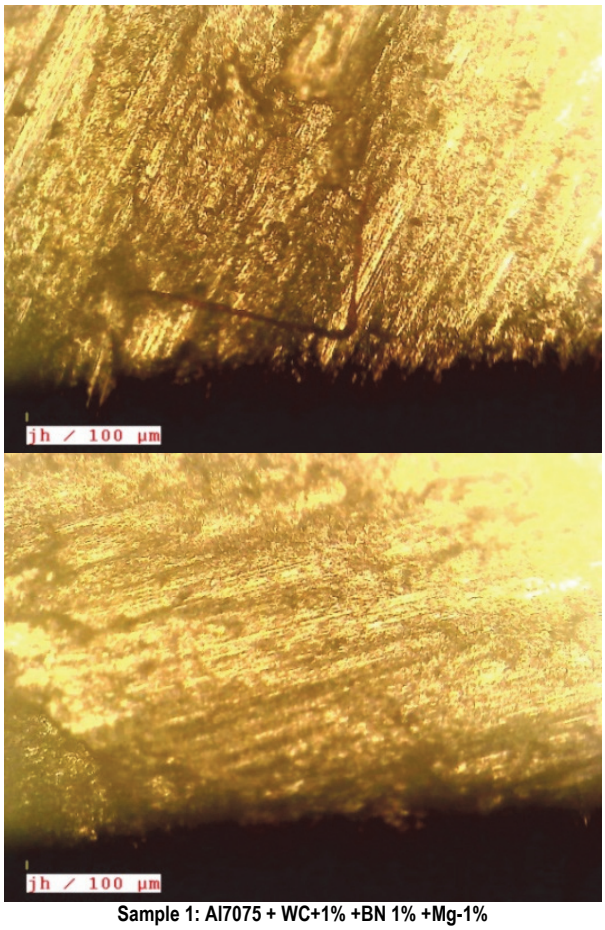

Sample 1: Al7075 + WC+1% +BN 1% +Mg-1%

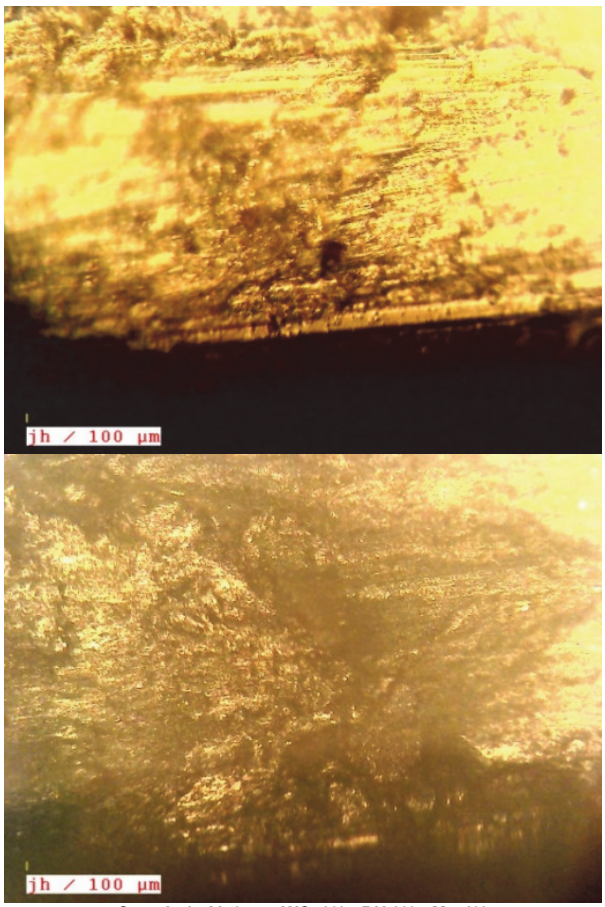

Sample 2: Al7075 + WC+3% +BN 3% +Mg-1%

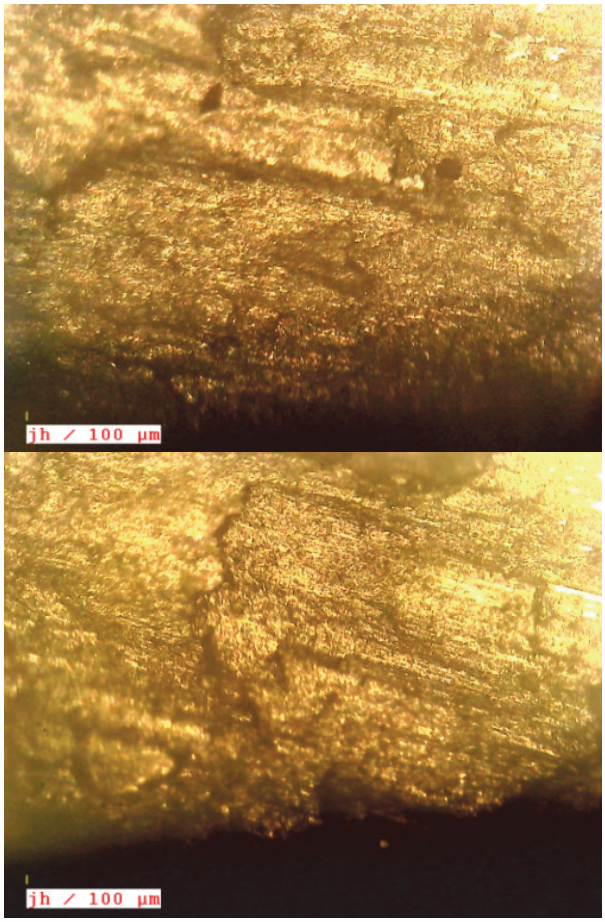

Sample 3: Al7075 + WC+1% +BN 1%+Mg-1%

Figure 12 SEM identification of Sample 1, Sample 2 and Sample 3

However, increasing the concentration of tungsten carbide can lead to a reduction in material removal rates during machining. While WC particles enhance the hardness and wear resistance of the composite, they also increase the material's overall hardness, resulting in higher cutting forces and tool wear, which decreases material removal rates. The effect of boron nitride on removal rates can be more complex, depending on factors such as cutting parameters, tool geometry, and machining conditions. Overall, optimizing the balance between these factors is crucial for achieving both desired surface finish and efficient material removal rates during machining of Al7075 composites with increased WC and BN compositions.

5 CONCLUSION

The present investigation employed the Taguchi technique combined with ANOVA to determine the ideal C.N.C. turning parameters for the AA7075 metal matrix under wet conditions. This study delves further into the topics of Taguchi analysis, parametric optimization, and surface roughness when turning carbide inserts of TNMG. Surface roughness parameters have a considerable influence on nose radius. The results facilitate the generation of the following conclusions.

- Roughness of around 0.718 µmm can be achieved with good surface quality when operated at fast speed, low feed rate, and large nose radius.
- The medium speed feed delivered a lesser material removal rate of 2.835 mm^3/min, and the greater nose radius increases the MRR; however, the timing's surface finish is extremely high.
- Lower TWR is achieved by the medium speed, feed rate, and greater nose radius at the minimum tool removal rate of 0.0005 grams. However, the timing's surface polish is slightly high.The very low wear rate of Al7075+ BN -5% + WC -5% + Mg -1% has been found to be the lowest wear rate observed on this ratio during the span of the experiment.
- Increasing tungsten carbide (WC) and boron nitride (BN) concentrations in Al7075 composites enhance surface smoothness due to improved hardness and lubrication. However, this may decrease material removal rates, particularly with higher WC levels, as it elevates cutting forces and tool wear. Balancing these factors is crucial for optimizing machining efficiency in Al7075 composites with heightened WC and BN contents.
- Several limitations are observed. Although increasing concentrations of Tungsten Carbide (WC) and Boron Nitride (BN) improve hardness and lubrication, they increase cutting forces and tool wear, lowering material removal rate. The research also solely used wet machining settings, which may not accurately reflect performance in dry or MQL situations. Focussing on individual process parameters hampers generalisations across machining settings or composite compositions. The findings may be more applicable if more situations and long-term tool performance are studied.

Acknowledgments

The authors extend their gratitude to their Research Supervisors and Technicians for their invaluable guidance and technical support throughout the research. Additionally, the authors wish to acknowledge the contributions of their co-authors in supporting this research project.

6 REFERENCES

[1] Alaneme, K. O. & Sanusi (2015). Microstructural characteristics, mechanical and wear behaviour of aluminium matrix hybrid composites reinforced with alumina, rice husk ash and graphite. *Engineering Science and Technology, an International Journal*, *18*(3), 1-7. https://doi.org/10.1016/j.jestch.2015.02.002

[2] Baradeswaran, A. & Perumal, E. (2014). Study on mechanical and wear properties of Al 7075/Al2O3/graphite hybrid composites. *Composites Part B: Engineering*, *56*, 464-471. https://doi.org/10.1016/j.compositesb.2013.08.093

[3] Baradeswaran, B, Vettivel, S. C., Perumal, A. E., Selvakumar, R., & Issac, R. F. (2014). Experimental investigation on mechanical behaviour, modelling and optimization of wear parameters of B4C and graphite reinforced aluminium hybrid composites. *Materials & Design*, *63*, 620-632. https://doi.org/10.1016/j.matdes.2014.05.072

[4] Chuandong, W., Kaka, M., Jialu, W., Pan, F., Guoqiang, L., Fei, C., Qiang, S., Lianmeng, Z., Schoenung, J. M., & Lavernia, E. J. (2016). Influence of particle size and spatial distribution of B4C reinforcement on the microstructure and mechanical behavior of precipitation strengthened Al alloy matrix composites. *Materials Science and Engineering: A*, *675*, 421-430. https://doi.org/10.1016/j.msea.2016.08.019

[5] Deaquino-Lara, R., Gutiérrez-Castañeda, E., Estrada-Guel, I., Hinojosa-Ruiz, G., García-Sánchez, E., Herrera-Ramírez, J M., Pérez-Bustamante, R., & Martínez-Sánchez, R. (2014). Structural characterization of aluminium alloy 7075-graphite composites fabricated by mechanical alloying and hot extrusion. *Materials & Desgin*, *53*, 1104-1111. https://10.1016/j.matdes.2013.07.087

[6] Deaquino-Lara, R., Soltani, N., Bahrami, A., Gutiérrez-Castañeda, E., García-Sánchez, E., & Hernandez-Rodríguez, M. (2015). Tribological characterization of Al7075-graphite composites fabricated by mechanical alloying and hot extrusion. *Materials & Desgin*, *67*, 224-231. https://doi.org/10.1016/j.matdes.2014.11.046

[7] Ezatpour, H. R., Parizi, M. T., Sajjadi, S. A., Ebrahimi, G. R., & Chaichi, A. (2016). Microstructure mechanical analysis and optimal selection of 7075 aluminum alloy based composite reinforced with alumina nanoparticles. *Materials Chemistry and Physics*, *178*(1), 119-127. https://doi.org/10.1007/s12666-016-0831-6

[8] Flores-Campos, R., Mendoza-Ruiz, D. C., Amézaga-Madrid, P., Estrada-Guel, I., Miki-Yoshida, M., Herrera-Ramírez, J. M., & Martínez-Sánchez, R. (2010). Microstructural and mechanical characterization in 7075 aluminum alloy reinforced by silver nanoparticles dispersion. *Journal of Alloys and Compounds*, *495*(2), 394-398. https://doi.org/10.1016/j.jallcom.2010.01.017

[9] Hernández-Martínez, S. E., Cruz-Rivera, J. J., Garay-Reyes, C. G., Elias-Alfaro, C. G., Martínez-Sánchez, R., & Hernández-Rivera, J. L. (2015). Application of ball milling in the synthesis of AA 7075-ZrO_2 metal matrix nanocomposite. *Powder Technology*, *284*, 40-46. https://doi.org/10.1016/j.powtec.2015.06.024

[10] Jiang, J. & Wang, Y. (2015). Microstructure and mechanical properties of the reformed cylindrical part of 7075 aluminum matrix composite reinforced with nano-sized SiC particles. *Materials & Design*, *79*, 32-41. https://doi.org/10.1016/j.matdes.2015.04.041

[11] Karunesh, G. & Manjunath, Y. J. (2016). Determination of mechanical properties of Aluminum Alloy (7075) reinforced with Aluminum oxide (Al2O3). *International Journal of Engineering Research*, *5*(6), 1129-1254. https://doi.org/10.1108/IJERA.2016.08.010

[12] Kumaravel, S., Mohanraj, D., & Channankaiah (2015). Production and Mechanical Properties of Fly ash and Basalt ash reinforced Al 6061 composites. *Procedia Engineering*, *16*, 10-15. https://doi.org/10.1016/j.matdes.2015.04.008

[13] Mindivan, H., Kayali, E. S., & Cimenoglu, H. (2007). Tribological behavior of squeeze cast aluminum matrix composites. *Wear*, *265*, 645-654. https://doi.org/10.1016/j.wear.2007.01.021

[14] Narasaraju, G. & Raju, D. L. (2015). Characterization of Hybrid Rice Husk and Fly ash-Reinforced Aluminium alloy (AlSi10Mg) Composites. *Materials Today: Proceedings*, *2*(4-5), 3056-3064. https://doi.org/10.1016/j.matpr.2015.07.353

[15] Raghavendra, N. & Ramamurthy, V. S. (2015). Tribological characterization of Al7075/Al2O3/SiC reinforced hybrid particulate metal matrix composite. *Tribology - Materials, Surfaces & Interfaces*, *4*(3), 113-127. https://doi.org/10.1179/1751584X15Y.0000000005

[16] Singla, D. & Mediratta, S. R. (2013). Evaluation of Mechanical Properties of Al7075-Fly Ash Composite Material. *International Journal of Innovative Science Engineering and Technology*, *2*(1), 951-959. https://doi.org/10.15680/IJIRSET.2013.0207030

[17] Saravanan, S. D. & Kumar, M. S. (2013). Effect of mechanical properties on rice husk ash reinforced aluminum alloy (AlSi10Mg) matrix composites. *Procedia Engineering*, *64*, 1505-1513. https://doi.org/10.1016/j.proeng.2013.09.231

[18] Veeresh Kumar, G. B., Rao, C. S. P., Selvaraj, N., & Bhagyashekar, M. S. (2010). Studies on Al6061-SiC and Al7075-Al2O3 Metal Matrix Composites. *Journal of Minerals and Materials Characterization and Engineering*, *9*(1), 43-55. https://doi.org/10.4236/jmmce.2010.91004

[19] Baradeswaran, A. & Perumal, E. (2014). Wear and mechanical characteristics of Al 7075/graphite composites. *Composites Part B: Engineering*, *56*, 472-476. https://doi.org/10.1016/j.compositesb.2013.08.094

[20] Bejaxhin, B. H., Paulraj, G., & Prabhakar, M. (2019). Inspection of casting defects and grain boundary strengthening on stressed Al6061 specimen by NDT method and SEM micrographs. *Journal of Materials Research & Technology*, *8*(3), 2674-2684. https://doi.org/10.1016/j.jmrt.2019.03.019

[21] Brucely, Y., Shaji, Y. C., Bejaxhin, A. B. H., & Abeens, M. (2022). Online acoustic emission measurement of tensile strength and wear rate for AA8011-TiC-ZrB2 hybrid composite. *Surface Topography: Metrology and Properties*, *10*(4), 045009. https://doi.org/10.1088/2051-672X/ac61fb

[22] Priya, C. B., Ramkumar, K., Vijayan, V., & Bejaxhin, A. B. H., (2022). Wear Studies on Mg-5Sn-3Zn-1Mn-xSi Alloy and Parameters Optimization Using the Integrated RSM-GRGA Method, Silicon. https://doi.org/10.1007/s12633-022-02243-z

[23] Rao, V., Periyaswamy, P., Bejaxhin, A. B. H., Naveen, E., Ramanan, N., & Teklemariam, A. (2022). Wear Behavioral Study of Hexagonal Boron Nitride and Cubic Boron Nitride-Reinforced Aluminum MMC with Sample Analysis. *Journal of Nanomaterials*, 7816372. https://doi.org/10.1155/2022/7816372

[24] Chandramohan, P., Siva Rangar, A., Joshua Kingsly, J., Bovas Herbert Bejaxhin, A., &Ramanan, N. (2023). Investigation of corrosion and wear behavior of Al-SiC composite. *Materials Today: Proceedings*. https://doi.org/10.1016/j.matpr.2023.03.440

[25] Šarić, T., Vukelić, Đ., Šimunović, K., Svalina, I., Tadić, B., Prica, M., & Šimunović, G. (2020). Modelling and Prediction of Surface Roughness in CNC Turning Process using Neural Networks. *Tehnički vjesnik*, *27*(6), 1923-1930. https://doi.org/10.17559/TV-20200818114207

[26] Khelfaoui, F., Mohammed, A. Y., Septi, B., Hanane, B., & Nourdine, O. (2023). Minimizing Tool Wear, Cutting Temperature and Surface Roughness in the Intermittent Turning of AISI D3 Steel Using the DF and GRA Method. *Tribology in Industry*, *45*(1), 89-101. https://doi.org/10.24874/ti.1395.10.22.01

[27] Vukelić, M., Radojević, M., & Mandić, A. (2022). Modelling surface roughness in finish turning as a function of cutting tool geometry using the response surface method, Gaussian process regression and decision tree regression. *Advances in Production Engineering & Management*, *17*(3), 442-454. https://doi.org/10.14743/apem2022.3.442

[28] Milosevic, A., Simunovic, G., Kanovic, Ž., Simunovic, K., Santosi, Ž., Sokac, M., & Vukelic, Đ. (2024). Comprehensive evaluation of dimensional deviation, flank wear, surface roughness and material removal rate in dry turning of C45 steel. *Facta Universitatis, Series: Mechanical Engineering*, *22*(4), 547-566. https://doi.org/10.22190/FUME240403024M

Contact information:

Mr. R. PARTHIBAN, Assistant Professor
(Corresponding author)
Department of Mechanical Engineering,
Mother Terasa College of Engineering and Technology,
622102 Pudukkottai, India
E mail: r.parthibanyugam@gmail.com

Dr. U. NATARAJAN, Professor - Mechanical
Government College of Engineering,
Srirangam, Trichy, India
E-mail: nattu33@gmail.com

Dr. A. KUMARAVADIVEL, Professor - Mechanical
Department of Mechanical Engineering,
Sir Issac Newton College of Engineering and Technology,
Nagapattinam, India
E-mail: poojaku2003@yahoo.co.in